Glass Fragility and Atomic Ordering on the Intermediate and Extended Range

Philip S. Salmon,[1] Adrian C. Barnes,[2] Richard A. Martin,[1] and Gabriel J. Cuello[3]
[1]*Department of Physics, University of Bath, Bath BA2 7AY, United Kingdom*
[2]*HH Wills Physics Laboratory, Royal Fort, University of Bristol, BS8 1TL, United Kingdom*
[3]*Institut Laue-Langevin, Boîte Postale 156, F-38042, Grenoble Cédex 9, France*
(Received 22 March 2006; published 13 June 2006)

The relation between the fragility of glass-forming systems, a parameter which describes many of their key physical characteristics, and atomic scale structure is investigated by using neutron diffraction to measure the topological and chemical ordering for germania, or GeO_2, which is an archetypal strong glass former. We find that the ordering for this and other tetrahedral network-forming glasses at distances greater than the nearest neighbor can be rationalized in terms of an interplay between the relative importance of two length scales. One of these is associated with an intermediate range, the other with an extended range and, with increasing glass fragility, it is the extended range ordering which dominates.

DOI: 10.1103/PhysRevLett.96.235502 PACS numbers: 61.43.Fs, 61.12.Ld

An essential prerequisite for understanding the nature of the glass transition is unambiguous experimental information on the atomic scale structure of glass-forming systems from the liquid to the glassy phase. Since these systems can be classified as ''strong'' or ''fragile,'' a taxonomy that rationalizes several different characteristics of liquid relaxation [1] and which can usefully be extended to the glassy phase [2,3], it is particularly important to appreciate the concomitant differences in underlying structure, especially on the *long* length scales that determine many important aspects of supercooled liquid and glass phenomenology [4]. Recently, the topological and chemical ordering in two network-forming AX_2 glasses was examined, namely $ZnCl_2$ and $GeSe_2$, and at distances greater than the nearest-neighbor, *two* length scales associated with the atomic ordering were identified [5]. One of these is associated with an *intermediate* range and manifests itself by the appearance in the measured diffraction patterns of a first-sharp diffraction peak (FSDP) at a scattering vector $k_{\mathrm{FSDP}} \approx 1$ Å^{-1}. The other is associated with an *extended* range which has a periodicity given by $\approx 2\pi/k_{\mathrm{PP}}$ where k_{PP} is the position of the principal peak at ≈ 2.1 Å^{-1}. It is therefore crucial to understand how this ordering affects the system properties; e.g., in the case of network-forming ionic melts the density fluctuations relax much more slowly on length scales associated with the FSDP compared with the principal peak [6]. In particular, what distinguishes the structure of a strong glass such as silica (SiO_2) or germania (GeO_2) from that of $ZnCl_2$ and $GeSe_2$ which are much more ''intermediate'' in character given that the dominant structural motif in all these systems is the $A(X_{1/2})_4$ tetrahedron?

We have therefore taken advantage of advances in neutron diffraction instrumentation [7] to apply the powerful method of isotopic substitution [5,8] to make the first accurate measurement of the topological and chemical ordering for an archetypal *strong* network-forming glass, namely GeO_2. Specifically, we measured the full set of Bhatia-Thornton [9] partial structure factors, $S_{IJ}^{\mathrm{BT}}(k)$, where I and J denote either the number density, N, or concentration, C, of species in the system. These functions separate the number density from the concentration fluctuations and hence information on the topological order described by $S_{\mathrm{NN}}^{\mathrm{BT}}(k)$ from information on the chemical order described by $S_{\mathrm{CC}}^{\mathrm{BT}}(k)$. The correlation between the number and concentration fluctuations is described by $S_{\mathrm{NC}}^{\mathrm{BT}}(k)$ [10]. Although these or related functions have previously been estimated for GeO_2 by combining x-ray and neutron diffraction methods, the results are prone to systematic error and even in the most recent work significant unphysical features can be identified [11–13]. Moreover, the results have not allowed for a detailed investigation of the glass structure at distances beyond the nearest neighbor.

The glasses were made by heating ≈1.35 g of powdered $^{\mathrm{nat}}GeO_2$ (99.9999% purity; nat denotes the natural isotopic enrichment), $^{70}GeO_2$ (97.22% enrichment) or $^{73}GeO_2$ (95.51% enrichment) contained in platinum crucibles (supported by alumina crucibles) in air at 1400 °C. After ≈2 h, the crucibles were removed from the furnace and placed on a copper block to cool to room temperature. The transparent, colorless samples are hygroscopic and were therefore stored under dry conditions. The neutron scattering lengths [14], taking into account the isotopic enrichments, are $b(^{\mathrm{nat}}\mathrm{Ge}) = 8.185(20)$, $b(^{70}\mathrm{Ge}) = 9.94(10)$, $b(^{73}\mathrm{Ge}) = 5.17(4)$, $b(\mathrm{O}) = 5.803(4)$ fm and the atomic number density is 0.0629(3) Å^{-3}. The diffraction experiments were made at 25(1) °C using the D4C instrument (ILL, Grenoble) [7] with an incident neutron wavelength of 0.499 91(2) Å. The data analysis followed the procedure described elsewhere [5,8] and the results for $^{\mathrm{nat}}GeO_2$ are in good agreement with previous measurements [15]. The $S_{IJ}^{\mathrm{BT}}(k)$ were obtained from the measured total structure factors by direct inversion of the scattering matrix [8] and, as shown in Fig. 1, all show a first-sharp diffraction peak at $k_{\mathrm{FSDP}} \approx 1.53$ Å^{-1} that is most prominent for $S_{\mathrm{NN}}^{\mathrm{BT}}(k)$. The associated intermediate range order [16] has a periodicity

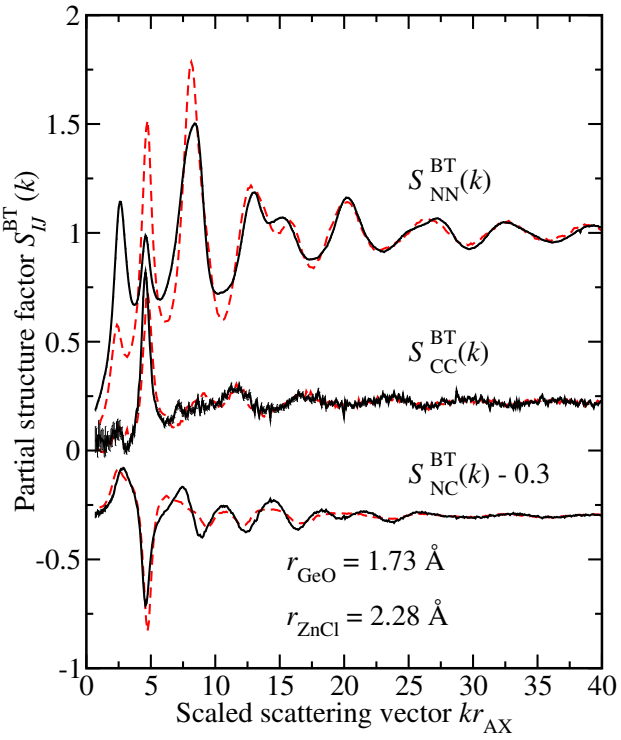

FIG. 1 (color online). The measured Bhatia-Thornton partial structure factors, $S_{IJ}^{BT}(k)$, for glassy GeO_2 (solid curves with vertical error bars—the latter are comparable to the curve thickness at most k values) and $ZnCl_2$ [broken curves (red online)] plotted as a function of the scaled scattering vector kr_{AX} where r_{AX} is the separation of unlike nearest neighbors. In the case of GeO_2 each function has a FSDP at $k \approx 1.53$ Å^{-1} or $kr_{AX} \approx 2.65$.

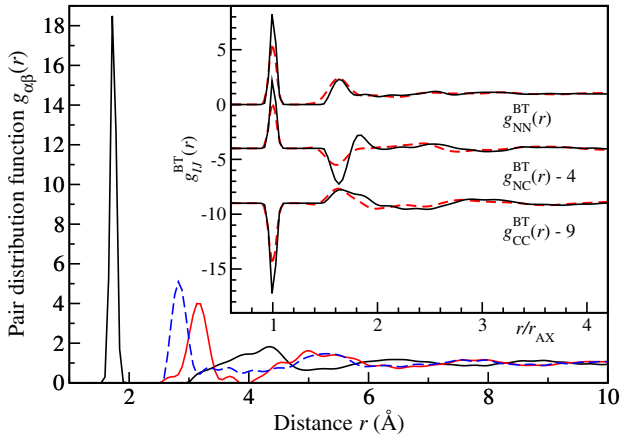

FIG. 2 (color online). The measured partial pair-distribution functions $g_{GeO}(r)$ (solid black curve), $g_{GeGe}(r)$ [light solid curve (red online)] and $g_{OO}(r)$ [broken curve (blue online)] for glassy GeO_2. The inset shows the Bhatia-Thornton partial pair-distribution functions, $g_{IJ}^{BT}(r)$, for GeO_2 (solid black curves) and $ZnCl_2$ [broken curves (red online)] plotted as a function of the scaled distance, r/r_{AX}, which ensures that the first peak positions are superimposed. The $g_{IJ}^{BT}(r)$ were obtained from the $g_{\alpha\beta}(r)$ by using the relations [26] $g_{NN}^{BT}(r) = c_A^2 g_{AA}(r) + c_X^2 g_{XX}(r) + 2c_A c_X g_{AX}(r)$, $g_{CC}^{BT}(r) = c_A c_X [g_{AA}(r) + g_{XX}(r) - 2g_{AX}(r)]$ and $g_{NC}^{BT}(r) = c_A[g_{AA}(r) - g_{AX}(r)] - c_X[g_{XX}(r) - g_{AX}(r)]$ where $c_A = 1/3$ and $c_X = 2/3$.

$2\pi/k_{FSDP}$ and coherence length $2\pi/\Delta k_{FSDP}$ where Δk_{FSDP} is the full width at half maximum of the FSDP. In the case of $S_{NN}^{BT}(k)$, the periodicity and coherence length take values of 4.13(3) and 8.98(13) Å, respectively.

The partial pair-distribution functions, $g_{GeO}(r)$, $g_{GeGe}(r)$, and $g_{OO}(r)$, which give a measure of the probability of finding two atoms of type α and β at a distance r apart, are plotted in Fig. 2. They were obtained by using the procedure described elsewhere [5] and it was confirmed that their back Fourier transforms agree with the measured partial structure factors. A structure based on tetrahedral $Ge(O_{1/2})_4$ building blocks is thus deduced in which there are 3.8(1) Ge-O nearest-neighbors at $r_{GeO} = 1.73(1)$ Å and the O-O distance is $r_{OO} = 2.83(1)$ Å i.e., the ratio $r_{OO}/r_{GeO} = 1.636(11)$ is close to the ideal tetrahedral ratio of $\sqrt{8/3} = 1.633$. The tetrahedra share corners to give 4.1(2) Ge-Ge nearest-neighbors at 3.16(1) Å and there is an average of 6.7(1) O-O nearest-neighbors for $2.58 \leq r(\text{Å}) \leq 3.13$. The packing fraction of oxygen atoms in tetrahedral units, calculated from r_{OO} and the atomic number density, is 0.498(5). As in several other diffraction studies [15,17] the measured Ge-O coordination number is systematically less that four owing to the finite k-space resolution function of the diffractometer for which a correction was not made [18]. The mean intertetrahedral Ge-Ô-Ge bond angle of 132(2)°, as obtained from the first Ge-O and Ge-Ge peak positions, is consistent with the literature [13,19,20]. The corresponding Bhatia-Thornton partial pair-distribution functions $g_{NN}^{BT}(r)$, $g_{CC}^{BT}(r)$, and $g_{NC}^{BT}(r)$ are shown in the inset to Fig. 2. Here $g_{NN}^{BT}(r)$ describes the sites of the scattering nuclei but does not distinguish between the chemical species that decorate those sites, $g_{CC}^{BT}(r)$ describes the chemical ordering and has positive or negative peaks when there is a preference for like or unlike neighbors, respectively, and $g_{NC}^{BT}(r)$ describes the correlation between sites and their occupancy by a given chemical species.

The structure of the intermediate glass $ZnCl_2$ is also based on corner sharing $A(X_{1/2})_4$ motifs [5] which are, however, much more densely packed than for GeO_2 with an anion packing fraction of 0.635(5) and a mean intertetrahedral Zn-Ĉl-Zn bond angle of 111(1)°. As shown in Figs. 1 and 2, the concomitant differences in structure manifest themselves most prominently in the number-number partial structure factor, $S_{NN}^{BT}(k)$, which describes the topological ordering and hence the relative arrangement of the tetrahedra. In real space, sharper first peaks are observed for GeO_2 compared with $ZnCl_2$ (see Fig. 2), in keeping with the higher vibrational frequencies observed in Raman spectroscopy experiments [21,22]. Structural differences also appear on the intermediate range $r/r_{AX} \approx 1.4$–4 where r_{AX} is the separation of unlike nearest neighbors.

To examine further the differences between the topological and chemical ordering at distances greater than the nearest neighbor, it is useful to consider the functions $\ln|rh_{IJ}^{\mathrm{BT}}(r)|$, where $h_{\mathrm{NN}}^{\mathrm{BT}}(r) = g_{\mathrm{NN}}^{\mathrm{BT}}(r) - 1$, $h_{\mathrm{CC}}^{\mathrm{BT}}(r) = g_{\mathrm{CC}}^{\mathrm{BT}}(r)$, $h_{\mathrm{NC}}^{\mathrm{BT}}(r) = g_{\mathrm{NC}}^{\mathrm{BT}}(r)$. The rationale is that for systems described by simple model pair-potentials, the $rh_{IJ}^{\mathrm{BT}}(r)$ have analytical asymptotic large-r forms [23,24] which can therefore act as a benchmark for understanding the origin of extended range ordering in more complicated systems that involve three-body potentials. For example, all of the $rh_{IJ}^{\mathrm{BT}}(r)$ for a binary ionic system, described by pair potentials with short-ranged repulsive and long-ranged Coulomb terms, will eventually decay exponentially with identical decay lengths [23]. When van der Waals (dispersion) forces with a term proportional to r^{-6} are also included, the $rh_{IJ}^{\mathrm{BT}}(r)$ functions should eventually decay with different power-law dependences [25]. The $h_{IJ}^{\mathrm{BT}}(r)$ were obtained by spline fitting and Fourier transforming the $S_{IJ}^{\mathrm{BT}}(k)$ after the low-k data points ($k \leq 0.45$ Å^{-1}) were extrapolated to zero by assuming $S_{IJ}^{\mathrm{BT}}(k) \propto k^2$ [26] and a Lorch modification function was applied [17]. The resultant $\ln|rh_{IJ}^{\mathrm{BT}}(r)|$ functions for both glasses were brought into alignment at large distances by plotting the results for GeO_2 in terms of the scaled distance $r' = [k_{\mathrm{PP}}\mathrm{GeO}_2)/k_{\mathrm{PP}}(\mathrm{ZnCl}_2)]r = 1.267r$ where $k_{\mathrm{PP}}(\mathrm{GeO}_2) = 2.66(1)$ and $k_{\mathrm{PP}}(\mathrm{ZnCl}_2) = 2.10(1)$ Å^{-1}.

The N-N pair-distribution function for each glass has greater complexity than the N-C and C-C functions over a wide range of distances and decays more rapidly at lower-r values. Also, the N-N function for the intermediate glass appears to have less complexity on the intermediate range compared with the strong glass. Intriguingly, all of the functions for *both* glasses show extended range ordering at large-r values which decays exponentially with a common decay length and a periodicity $2\pi/k_{\mathrm{PP}}$ that is comparable to the diameter of the larger (electronegative) species. These decay lengths, r_{decay} and r'_{decay}, take values ≈ 5 Å and were estimated by fitting the repeated maxima at large distances in Fig. 3, that are least sensitive to the details of any smoothing procedure, to the straight line $\ln|rh_{IJ}^{\mathrm{BT}}(r)| = -r/r_{\mathrm{decay}} + \text{constant}$ ($ZnCl_2$) or $\ln|r'h_{IJ}^{\mathrm{BT}}(r')| = -r'/r'_{\mathrm{decay}} + \text{constant}$ (GeO_2). The decay lengths thus deduced represent *lower* limits owing to the k-space resolution function of the diffractometer [18] that was, however, the *same* for both glasses. Thus, although GeO_2 and $ZnCl_2$ are generic covalent and ionic systems, respectively, the extended range ordering shows a communality that is independent of the details of the bonding scheme.

To investigate the relation between the structure of GeO_2 and other *strong* network-forming AX_2 glasses, the total structure factor $F_{\mathrm{Si}}(k)$ for SiO_2 was measured in the *same* neutron diffraction experiment used to obtain the partial structure factors for GeO_2. Silica is often regarded as the canonical network-forming glass and is of wide scientific and technological significance [1,27]. The measured $F_{\mathrm{Si}}(k)$ is compared in Fig. 4 with its reconstruction, $F_{\mathrm{Si}}^{\mathrm{rec}}(k)$, from the measured $S_{IJ}^{\mathrm{BT}}(k)$ for glassy germania. The structure of silica is also based on an open network of corner sharing $A(X_{1/2})_4$ tetrahedra, where the nearest-neighbor Si-O and O-O distances are 1.60(1) and 2.62(1) Å, respectively, although the packing fraction of the oxygen atoms is smaller at 0.417(5) and the mean intertetrahedral bond angle, Si-Ô-Si, is larger at 148° [19]. The relative arrangement of the $A(X_{1/2})_4$ tetrahedra is therefore different and manifests itself on both the intermediate and extended range as shown by a higher and sharper FSDP in $F_{\mathrm{Si}}(k)$ compared with $F_{\mathrm{Si}}^{\mathrm{rec}}(k)$ together with a lower and broader principal peak. The same general features nevertheless occur in the total structure factors for both strong glasses.

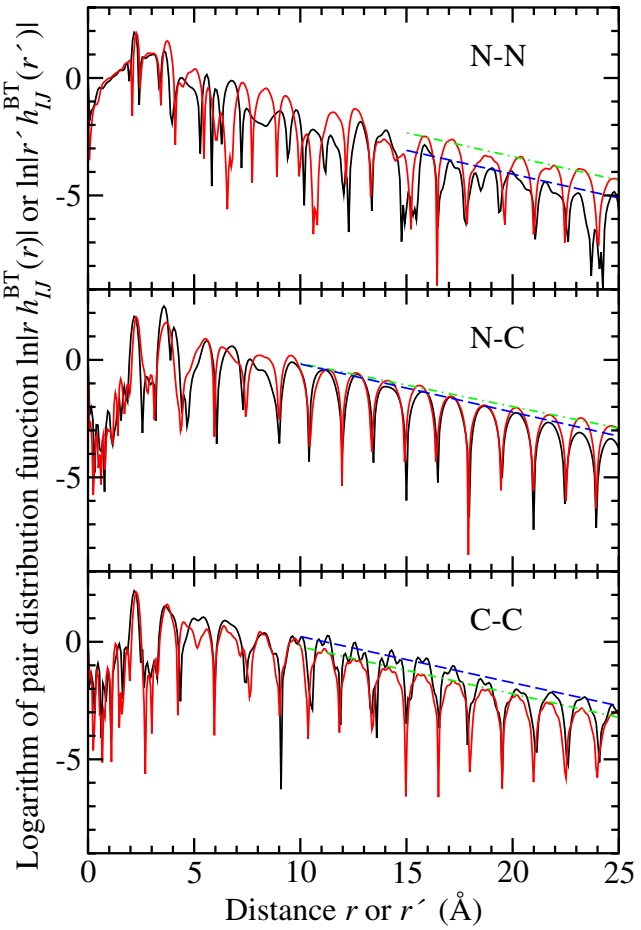

FIG. 3 (color online). Decay of the Bhatia-Thornton partial pair-distribution functions for glassy GeO_2 and $ZnCl_2$ as shown by plotting $\ln|r'h_{IJ}^{\mathrm{BT}}(r')|$ vs r' (dark solid black curves for GeO_2) or $\ln|rh_{IJ}^{\mathrm{BT}}(r)|$ vs r [light solid curves (red online) for $ZnCl_2$] [24] where the scaled distance, r', is related to the actual distance by $r' = 1.267r$. The decay length for the N-N, N-C, and C-C functions is 4.9(7), 4.9(2), 5.1(4) Å for GeO_2 and 5.0(4), 5.4(2), and 5.0(1) Å for $ZnCl_2$, respectively, and was obtained from the fitted straight lines given by the broken blue (GeO_2) or chained green ($ZnCl_2$) curves. The quoted r'_{decay} values for GeO_2 are related to the actual decay lengths by $r'_{\mathrm{decay}} = 1.267r_{\mathrm{decay}}$.

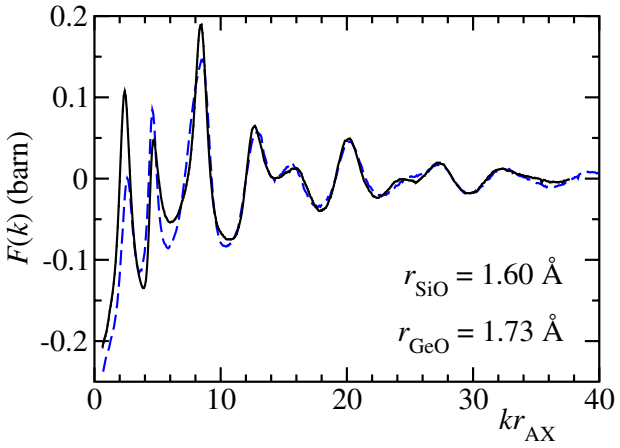

FIG. 4 (color online). The measured total-structure factor for SiO_2, $F_{Si}(k)$, (solid curve—the error bars are smaller than the curve thickness) is compared with its reconstruction, $F_{Si}^{rec}(k)$, (broken curve) from the measured partial structure factors for GeO_2 (see Fig. 1) where $F_{Si}^{rec}(k)/\text{barn} = 0.2758(3)[S_{NN}^{BT}(k) - 1] + 0.00608(3)[S_{CC}^{BT}(k)/c_A c_X - 1] - 0.1737(4)S_{NC}^{BT}(k)$ and the weighting factors are calculated from the scattering lengths and atomic fractions of Si and O [26]. Both data sets are plotted as a function of the scaled scattering vector kr_{AX}. The atomic number density of SiO_2 is 0.0665(2) $Å^{-3}$ and the coherent scattering length $b(\text{Si}) = 4.1491(10)$ fm.

Finally, polyamorphic phase transitions are often associated with a distinct change in the structure of a liquid or glass from strong to fragile with increase of density [27,28] and tetrahedrally bonded systems currently remain the most promising candidates for studying this phenomenon experimentally [28]. Furthermore, two or more competing length scales are built into simple model pair potentials that are used in calculations to examine the feasibility of liquid-liquid phase transitions [29,30]. The present results show that it is the relative importance of the FSDP and principal peak that most readily enables a distinction to be made between the diffraction patterns measured for the open tetrahedral network of the strong glass GeO_2 and the densely packed tetrahedral network of the intermediate glass $ZnCl_2$. When pressure is applied to GeO_2, diffraction experiments show that the principal peak gains in intensity and the FSDP disappears as the network first collapses and the germanium coordination number eventually increases [31]. For silica, the measured diffraction pattern features a more prominent FSDP and weaker principal peak (see Fig. 4) and much higher pressures are required to induce a network collapse compared to germania [21,31]. Hence there is a competition between the intermediate and extended range ordering in network AX_2 glasses that is won by the latter with increasing density.

We gratefully thank P. Palleau for help with the diffraction experiment, R. Evans and P. A. Madden for helpful discussions, A. C. Wright for providing his data for GeO_2, and the EPSRC for financial support.

[1] C. A. Angell, Science **267**, 1924 (1995).
[2] T. Scopigno, G. Ruocco, F. Sette, and G. Monaco, Science **302**, 849 (2003).
[3] V. N. Novikov and A. P. Sokolov, Nature (London) **431**, 961 (2004).
[4] C. A. Angell, J. Non-Cryst. Solids **73**, 1 (1985).
[5] P. S. Salmon, R. A. Martin, P. E. Mason, and G. J. Cuello, Nature (London) **435**, 75 (2005).
[6] M. Foley, M. Wilson, and P. A. Madden, Philos. Mag. B **71**, 557 (1995).
[7] H. E. Fischer, G. J. Cuello, P. Palleau, D. Feltin, A. C. Barnes, Y. S. Badyal, and J. M. Simonson, Appl. Phys. A **74**, S160 (2002).
[8] P. S. Salmon and I. Petri, J. Phys. Condens. Matter **15**, S1509 (2003).
[9] A. B. Bhatia and D. E. Thornton, Phys. Rev. B **2**, 3004 (1970).
[10] P. S. Salmon, Proc. R. Soc. A **437**, 591 (1992).
[11] P. Bondot, Acta Crystallogr., Sect. A. Cryst. Phys. Diffr. Theor. Gen. Crystallogr. **30**, 470 (1974).
[12] Y. Waseda, K. Sugiyama, E. Matsubara, and K. Harada, Mater. Trans., JIM **31**, 421 (1990).
[13] D. L. Price, M.-L. Saboungi, and A. C. Barnes, Phys. Rev. Lett. **81**, 3207 (1998).
[14] V. F. Sears, Neutron News **3**, 26 (1992).
[15] J. A. E. Desa, A. C. Wright, and R. N. Sinclair, J. Non-Cryst. Solids **99**, 276 (1988).
[16] P. S. Salmon, Proc. R. Soc. A **445**, 351 (1994).
[17] E. Lorch, J. Phys. C **2**, 229 (1969).
[18] D. I. Grimley, A. C. Wright, and R. N. Sinclair, J. Non-Cryst. Solids **119**, 49 (1990).
[19] J. Neuefeind and K.-D. Liss, Ber. Bunsenges Phys. Chem. **100**, 1341 (1996).
[20] L. Giacomazzi, P. Umari, and A. Pasquarello, Phys. Rev. Lett. **95**, 075505 (2005).
[21] D. J. Durben and G. H. Wolf, Phys. Rev. B **43**, 2355 (1991).
[22] C. H. Polsky, L. M. Martinez, K. Leinenweber, M. A. VerHelst, C. A. Angell, and G. H. Wolf, Phys. Rev. B **61**, 5934 (2000).
[23] R. J. F. Leote de Carvalho and R. Evans, Mol. Phys. **83**, 619 (1994).
[24] C. Grodon, M. Dijkstra, R. Evans, and R. Roth, J. Chem. Phys. **121**, 7869 (2004).
[25] R. Kjellander and B. Forsberg, J. Phys. A **38**, 5405 (2005).
[26] P. S. Salmon, J. Phys. Condens. Matter **17**, S3537 (2005).
[27] I. Saika-Voivod, P. H. Poole, and F. Sciortino, Nature (London) **412**, 514 (2001).
[28] P. H. Poole, T. Grande, C. A. Angell, and P. F. McMillan, Science **275**, 322 (1997).
[29] G. Franzese, G. Malescio, A. Skibinsky, S. V. Buldyrev, and H. E. Stanley, Nature (London) **409**, 692 (2001).
[30] E. A. Jagla, Phys. Rev. E **63**, 061501 (2001).
[31] M. Guthrie, C. A. Tulk, C. J. Benmore, J. Xu, J. L. Yarger, D. D. Klug, J. S. Tse, H.-k. Mao, and R. J. Hemley, Phys. Rev. Lett. **93**, 115502 (2004).